

The role of the reaction medium pH in the formation of nanocrystalline phases in the $\text{Bi}_2\text{O}_3\text{--P}_2\text{O}_5\text{--H}_2\text{O}$ system

Dmitry P. Elovikov^a, Alena A. Osminina^b

Grebenshchikov Institute of Silicate Chemistry, Russian Academy of Sciences, St. Petersburg, Russia

^asyncdima@mail.ru, ^balenaosminina3001@gmail.com

Corresponding author: Dmitry P. Elovikov, syncdima@mail.ru

ABSTRACT The work is devoted to studying the influence of pH values in an aqueous-salt medium on the formation of compounds in the $\text{Bi}_2\text{O}_3\text{--P}_2\text{O}_5\text{--H}_2\text{O}(\text{OH}^-, \text{H}^+)$ oxide system. It has been shown that in an acidic environment ($\text{pH} = 2$) at a temperature of 298 K, hexagonal BiPO_4 forms, while at pH values of 8 and 12, X-ray amorphous substances are produced. After hydrothermal treatment at 473 K in an aqueous-salt environment, a monoclinic modification of bismuth phosphate forms from hexagonal bismuth phosphate in an acidic environment, and nanometer-sized particles of crystalline compounds $\text{Bi}_3\text{O}(\text{OH})(\text{PO}_4)_2$ (with a crystallite size of about 62 nm) and Bi_2O_3 (with a crystallite size of about 70 nm) form in weakly alkaline and alkaline media. Using the method of thermodynamic calculation, the dependences of the equilibrium molar solubility of these crystalline compounds on the pH value of the aqueous-salt suspension were obtained. Thermodynamic calculations showed that the BiPO_4 compound is stable in the pH range from 0 to 5.8 at temperatures of 298 and 473 K. The pH range from 5.8 to 9.8 is characterized by the formation of the $\text{Bi}_3\text{O}(\text{OH})(\text{PO}_4)_2$ compound at 298 K, and a further increase in the pH value leads to the precipitation of Bi_2O_3 , BiOOH or $\text{Bi}(\text{OH})_3$, which are similar in solubility, at 298 and 473 K. The data obtained from thermodynamic calculations are consistent with experimental data on the stability boundaries of BiPO_4 , $\text{Bi}_3\text{O}(\text{OH})(\text{PO}_4)_2$, and Bi_2O_3 compounds.

KEYWORDS nanocrystals, BiPO_4 , $\text{Bi}_3\text{O}(\text{OH})(\text{PO}_4)_2$, influence of pH value, solubility, thermodynamic calculation, hydrothermal synthesis

ACKNOWLEDGEMENTS The work was supported by state assignment No. 1023032900322-9-1.4.3. Elemental analyses of samples were performed employing the equipment of the Engineering Center of the St. Petersburg State Institute of Technology. The X-ray structural studies of the samples were carried out using the DRON-8 diffractometer at the Ioffe Institute.

FOR CITATION Elovikov D.P., Osminina A.A. The role of the reaction medium pH in the formation of nanocrystalline phases in the $\text{Bi}_2\text{O}_3\text{--P}_2\text{O}_5\text{--H}_2\text{O}$ system. *Nanosystems: Phys. Chem. Math.*, 2024, **15** (3), 361–368.

1. Introduction

Low-temperature chemistry encompasses a wide variety of methods and approaches for synthesizing compounds and producing functional materials based on them [1–6]. Among the widely used and promising methods are precipitation and co-precipitation techniques [7–9], sol-gel methods [10–15], and hydrothermal treatment in various modifications [16–24]. Water and aqueous solutions often serve as the medium for heat and mass transfer during synthesis using these approaches. It is known that the composition of such a medium can significantly influence on the processes of compound formation [25–30], their structure and polymorphic transformations [31–35], the morphology of the resulting particles [36–39], crystallite sizes [40–43], and, consequently, the physicochemical and functional properties of the obtained compounds and materials. In this regard, it is pertinent to study the influence of various factors on the processes of compound formation, such as the composition of the aqueous solution, the concentration of soluble precursors, mineralizing additives, the sequence and conditions of mixing solutions, the presence and state of amorphous precursors [44–49], and the use of specific additional conditions: such as limiting mass transfer [6, 50], various physical impacts [51, 52], and the organization of reagent solution flows [53–55].

One of the important synthesis parameters reflected in this work is the pH value of solutions and suspensions, as well as its influence on the processes of oxide compound formation. For many low-temperature processes involving bismuth cation and phosphate anions, it is characteristic that a stable bismuth phosphate (with a hexagonal structure) precipitates at certain stages [56]. In some cases, associated with the formation of complex oxide compounds based on bismuth and phosphorus, this leads to kinetic hindrances (undesirable limiting factors of mass transfer) and the stable existence of BiPO_4 over a wide pH range [57]. Several studies have focused on the polymorphic transformations of simple compounds in the $\text{Bi}_2\text{O}_3\text{--P}_2\text{O}_5$ system [56, 58, 59] and the targeted synthesis of individual compounds: BiPO_4 or Bi_2O_3 . There are mentions of a new and promising compound for use in photocatalysis, $\text{Bi}_3\text{O}(\text{OH})(\text{PO}_4)_2$, obtained in this system [60, 61].

However, little attention has been paid to the thermodynamic analysis of the formation of complex compounds in the $\text{Bi}_2\text{O}_3\text{-P}_2\text{O}_5\text{-H}_2\text{O}(\text{OH}^-, \text{H}^+)$ system.

Due to the reasons listed above, this work is devoted to studying the influence of the pH value of the solution in the reaction medium on the formation of compounds in the $\text{Bi}_2\text{O}_3\text{-P}_2\text{O}_5\text{-H}_2\text{O}$ system, as well as the stability boundaries of these compounds, particularly, by using the thermodynamic calculations.

2. Experimental

For the synthesis, two solutions were initially prepared. The first solution was an acidic aqueous solution of bismuth nitrate, obtained by dissolving $\text{Bi}(\text{NO}_3)_3 \cdot 5\text{H}_2\text{O}$ (analytical grade) in a 6 M aqueous solution of HNO_3 (analytical grade). The second solution was prepared by dissolving a specified amount of NaOH (analytical grade) in 50 ml of distilled water, followed by the addition of a measured amount of $(\text{NH}_4)_2\text{HPO}_4$ (analytical grade). The mixing of the two solutions was carried out by the dropwise addition of the acidic bismuth nitrate solution into the alkaline ammonium phosphate solution under continuous stirring. The resulting suspensions with pH values of 2, 8, and 12 were stirred for 10 minutes at $T = 298$ K.

The hydrothermal treatment of the suspensions obtained at room temperature was carried out in a stainless steel autoclave with a Teflon liner (filling coefficient 0.8) at $T = 473$ K for 20 hours.

The samples, obtained both by precipitation and after hydrothermal treatment, were decanted by centrifugation (3500 rpm) for 30 minutes, washed with distilled water until $\text{pH} = 7$, dried at $T = 353$ K for 24 hours, and ground in an agate mortar.

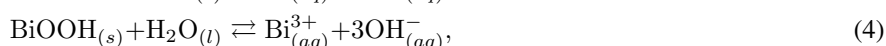
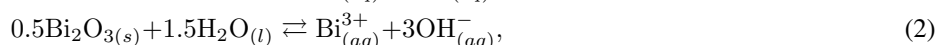
The samples were designated in the work according to the pH of the aqueous-saline suspension during precipitation: those obtained by the precipitation method were labeled as “pH = 2”, etc.; those obtained after hydrothermal treatment were labeled as “pH = 2(HTS)”, etc.

X-ray diffraction studies of the obtained samples were performed using the DRON-8 (8H) X-ray diffractometer (Russia) with CuK_α radiation in the 2θ range of $10 - 80^\circ$, with a step size of 0.0142° and a scanning speed of $3^\circ/\text{min}$. Qualitative analysis of the samples was performed using the ICSD PDF-2 database. The distribution of crystallites by size and the average weighted values of crystallite sizes were determined for the reflections with the maximum intensity.

For X-ray spectral microanalysis of the samples' composition, a scanning electron microscope Tescan Vega 3 SBH (Tescan, Czech Republic) with an Oxford Instruments INCA x-act attachment (United Kingdom) was used. Measurements were conducted in the range up to 20 keV.

3. Calculation

In aqueous-salt solutions saturated with relatively sparingly soluble solids $h\text{-BiPO}_4$, $c\text{-Bi}_2\text{O}_3$, $\text{Bi}(\text{OH})_3$, BiOOH , and $\text{Bi}_3\text{O}(\text{OH})(\text{PO}_4)_2$, the following heterogeneous equilibria are established:



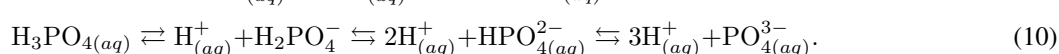
The thermodynamic constants of the specified heterogeneous equilibria are determined by the expressions:

$$K_S^0(1) = [a_{\text{Bi}^{3+}} \cdot X_{\text{Bi}^{3+}} \cdot a_{\text{PO}_4^{3-}} \cdot X_{\text{PO}_4^{3-}}]_T = \text{const}(T),$$

$$K_S^0(2-4) = [a_{\text{Bi}^{3+}} \cdot X_{\text{Bi}^{3+}} \cdot a_{\text{OH}^-}^3]_T = \text{const}(T),$$

$$K_S^0(5) = [a_{\text{Bi}^{3+}}^3 \cdot X_{\text{Bi}^{3+}}^3 \cdot a_{\text{OH}^-}^3 \cdot a_{\text{PO}_4^{3-}}^2 \cdot X_{\text{PO}_4^{3-}}^2]_T = \text{const}(T),$$

where K_S^0 is the thermodynamic solubility constant, $X_{\text{Bi}^{3+}}$ and $X_{\text{PO}_4^{3-}}$ – are the mole fractions of free cations Bi^{3+} and anions PO_4^{3-} , respectively. In an aqueous solution, depending on the pH value, the following homogeneous equilibria of water-soluble weak acids and bases are established:



Equilibria (6) – (9) are described by the corresponding stability constants of mononuclear hydroxo complexes of Bi(III) in an aqueous medium: $\beta_1, \beta_2, \beta_3, \beta_4 = f(T)$.

Equilibria (10) are described by the corresponding constants of the three-step dissociation of phosphoric acid: $K_1, K_2, K_3 = f(T)$.

The necessary values of the Gibbs free energy of formation for compounds were taken from the HSC 6.0 database. The Gibbs free energy of formation of the compound $\text{Bi}_3\text{O}(\text{OH})(\text{PO}_4)_2$ was calculated using the increment method based on data from reference [62]. Using these values, changes in the Gibbs free energy of processes were calculated, and subsequently, equilibrium constants, stability constants of mononuclear hydroxo complexes, and dissociation constants were calculated. By means of mathematical transformations described earlier in reference [63], the equilibrium molar solubility (S , mol/L) of sparingly soluble BiPO_4 , Bi_2O_3 , $\text{Bi}(\text{OH})_3$, BiOOH , and $\text{Bi}_3\text{O}(\text{OH})(\text{PO}_4)_2$ in the aqueous-salt suspension was calculated. The calculation was performed taking into account the mole fractions of water-soluble bound and free ions (equilibria (6) – (10)), the ionic strength of the solution (calculated for each composition point), the temperature dependence of the water autoprotolysis constant, and the temperature dependence of equilibria (1) – (4) and (6) – (10). For the calculation at 473 K, it was assumed that water is only in the liquid state.

4. Results and discussion

The results of X-ray diffraction studies of the obtained samples showed that the pH value and temperature play an important role in the formation processes of compounds in the $\text{Bi}_2\text{O}_3\text{-P}_2\text{O}_5\text{-H}_2\text{O}$ system. Thus, under precipitation conditions at room temperature (298 K) and a pH value of 2 of the aqueous-salt suspension, the appearance of reflections of crystalline BiPO_4 with a hexagonal ximengite-like structure can be observed (Fig. 1). With an increase in pH to 8 and 12, well-defined reflections of the crystalline compound are absent (Fig. 1a). This indicates the X-ray amorphous state of the obtained samples. Hydrothermal treatment at 473 K for 20 h of the aqueous-salt suspensions obtained at room temperature leads to the formation of new crystalline compounds (Fig. 1b). The results of elemental analysis of the obtained samples (Table 1) satisfy the stoichiometry of the crystalline compounds within the error of determination of Bi and P atoms.

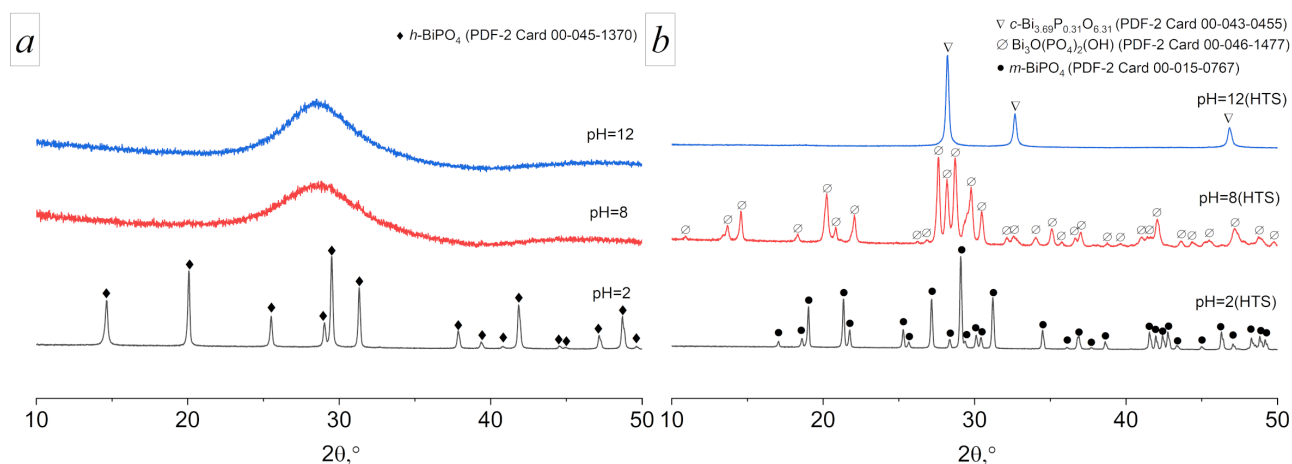


FIG. 1. Diffraction patterns obtained under different conditions (pH, T) of samples. a – 298 K, b – 473 K

During isothermal treatment under hydrothermal conditions of the aqueous-salt suspension with a pH of 2, containing particles of sparingly soluble crystalline BiPO_4 , a restructuring of the structure from hexagonal to a low-temperature monoclinic modification is observed, which is reflected in the change in the topology of the reflections (Fig. 1).

It is worth noting that the average crystallite sizes (weighted average) increase from 75 to 200 nm, while the average sizes of aggregated particles (length) increase from 1 to 1.5 μm . This indicates that even at room temperature under these conditions, there is active crystallite growth and the formation of large aggregates, the treatment of which under hydrothermal conditions leads to further growth in crystallite sizes. The similarity in morphology and particle sizes (on average 0.3 and 0.4 μm in width) may indicate that the polymorphic transformation $h\text{-BiPO}_4 \rightarrow m\text{-BiPO}_4$ occurs via a martensitic mechanism. The subsequent prolonged particle growth (on average 0.03 $\mu\text{m}/\text{h}$, Fig. 2) primarily affects the change in particle length and may be due to mass transfer processes limited in speed by the low ion concentration in the solution. This polymorphic transition was also noted in paper [59].

Hydrothermal treatment of aqueous-salt suspensions containing amorphous substances, obtained at room temperature under precipitation conditions at pH 8 and 12, leads to the formation of nanocrystalline compounds $\text{Bi}_3\text{O}(\text{OH})(\text{PO}_4)_2$ with a petitjeanite-like structure and $c\text{-Bi}_2\text{O}_3$ doped with phosphorus, respectively (Fig. 1). The weighted average particle sizes for the $\text{Bi}_3\text{O}(\text{OH})(\text{PO}_4)_2$ compound are approximately 200 nm for particles and approximately 62 nm for crystallites

TABLE 1. Results of X-ray diffraction studies and elemental analysis

| Designation of samples | Crystalline phase / Chemical formula in oxide form | Elemental analysis | | Chemical formula in oxide form according to elemental analysis |
|------------------------|---|--------------------|------|--|
| | | Bi | P | |
| pH = 2 | <i>h</i> -BiPO ₄ (Ximengite-like structure) 0.5[Bi ₂ O ₃ -P ₂ O ₅] | 50±1 | 50±2 | 0.5[Bi ₂ O ₃ -P ₂ O ₅] |
| pH = 8 | X-ray amorphous | 70±1 | 30±2 | 0.7Bi ₂ O ₃ -0.3P ₂ O ₅ |
| pH = 12 | X-ray amorphous | 88±1 | 12±2 | 0.9Bi ₂ O ₃ -0.1P ₂ O ₅ |
| pH = 2(HTS) | <i>m</i> -BiPO ₄ 0.5[Bi ₂ O ₃ -P ₂ O ₅] | 51±1 | 49±2 | 0.5[Bi ₂ O ₃ -P ₂ O ₅] |
| pH = 8(HTS) | Bi ₃ O(OH)(PO ₄) ₂ (Petitjeanite-like structure) 1.5[Bi ₂ O ₃ -0.7P ₂ O ₅ -0.3H ₂ O] | 63±1 | 37±2 | 1.5[Bi ₂ O ₃ -0.6P ₂ O ₅] |
| pH = 12(HTS) | <i>c</i> -Bi _{3.69} P _{0.31} O _{6.31} 1.8[Bi ₂ O ₃ -0.09P ₂ O ₅] | 87±1 | 13±2 | 1.8[Bi ₂ O ₃ -0.3P ₂ O ₅] |

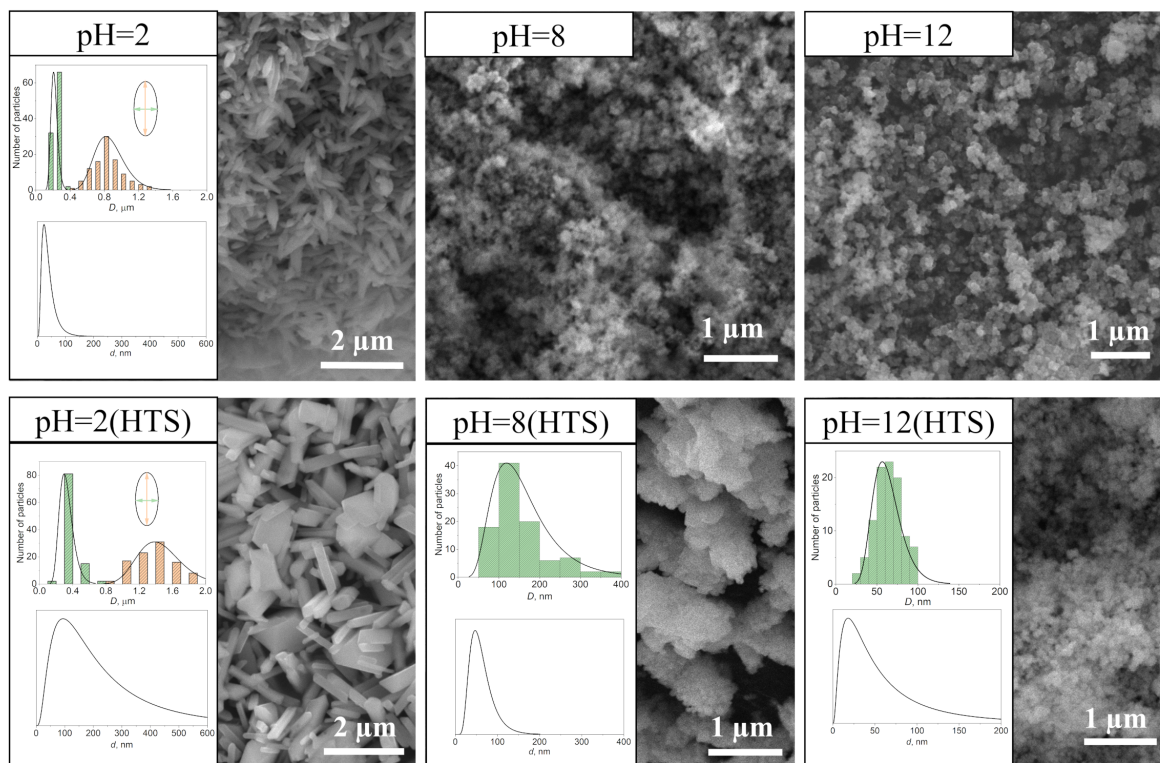


FIG. 2. Microphotographs of particles and lognormal dependences of the size distribution of particles and crystallites

(Fig. 2), indicating that the vast majority of particles are aggregates consisting of 30 – 40 interconnected crystallites. Spherical particles of the *c*- Bi_2O_3 compound, obtained by hydrothermal treatment of the X-ray amorphous precursor (Fig. 1b), are comparable in size to the crystallite sizes (weighted average is about 70 nm).

Thermodynamic calculations (Fig. 3) show that the compound BiPO_4 is formed and stable in the oxide system $\text{Bi}_2\text{O}_3\text{-P}_2\text{O}_5\text{-H}_2\text{O}(\text{OH}^-, \text{H}^+)$ within the pH range of 0 – 5.8 at temperatures of 298 and 473 K. This is consistent with the results obtained at pH = 2 in this study and with the results of obtaining BiPO_4 in acidic environments in several other studies [56,57,64,65]. It also aligns with the findings of study [66] where the formation of BiPO_4 was considered in the pH range of 0.5 – 4.0 at 298 K (mention of a white homogeneous mass) and 433 K. From pH 5.8 to 9.8, the most stable compound at 298 K is $\text{Bi}_3\text{O}(\text{OH})(\text{PO}_4)_2$. In this study, the compound $\text{Bi}_3\text{O}(\text{OH})(\text{PO}_4)_2$ was obtained by isothermal treatment under hydrothermal conditions of an amorphous substance with the following composition: $0.7\text{Bi}_2\text{O}_3\text{-}0.3\text{P}_2\text{O}_5$ in an aqueous-salt environment with a pH of 8. In the work of other authors, this compound was obtained at pH = 10, and in another study [61], the authors mention that they obtained it at a pH greater than 10. In this case, the calculation agrees with the data obtained in this study and satisfactorily agrees with the data from the works [60,61] within the error of calculating the Gibbs free energy of formation of $\text{Bi}_3\text{O}(\text{OH})(\text{PO}_4)_2$. The dashed line in Fig. 3 shows the region where freshly precipitated amorphous bismuth hydroxide, which is thermodynamically unstable, forms. At pH values greater than 10, bismuth oxides, hydroxides, and oxyhydroxides are approximately equally stable. However, according to the calculation, the lowest solubility is characteristic of bismuth hydroxide. In this study, at pH = 12, bismuth oxide doped with phosphorus of the composition $1.8\text{Bi}_2\text{O}_3\text{-}0.5\text{P}_2\text{O}_5$ was obtained. Apparently, this compound forms because in these conditions, the solution is dominated by water-soluble unbound phosphate anions. This fact may facilitate the incorporation of phosphorus into the structure. It is worth noting that the amorphous precursors also contain phosphorus atoms (Table 1).

5. Conclusions

It has been shown that the pH value of the medium significantly influences the formation of compounds in the aqueous-salt oxide system $\text{Bi}_2\text{O}_3\text{-P}_2\text{O}_5\text{-H}_2\text{O}(\text{OH}^-, \text{H}^+)$. Thus, at low pH values (pH = 2) and room temperature, hexagonal BiPO_4 is formed, while weakly alkaline and alkaline conditions promote the formation of X-ray amorphous substances. Hydrothermal treatment at 473 K leads to the polymorphic transformation of bismuth phosphate from hexagonal to monoclinic modification, as well as the formation of nanosized particles of crystalline compounds $\text{Bi}_3\text{O}(\text{OH})(\text{PO}_4)_2$ (with a crystal size of about 62 nm) and Bi_2O_3 (with a crystal size of about 70 nm) from amorphous precursors. Elemental analysis confirmed the correspondence of the chemical composition of the obtained crystalline compounds. By thermodynamic calculation, dependencies of the equilibrium molar solubility of identified compounds on the pH value of the aqueous-salt suspension were obtained, and for the compound $\text{Bi}_3\text{O}(\text{OH})(\text{PO}_4)_2$, such a dependence was obtained for the first time. Thermodynamic calculation showed that the compound BiPO_4 is stable in the pH range from 0 to 5.8 at temperatures of 298 and 473 K. The pH range from 5.8 to 9.8 is characterized by the stability of the compound $\text{Bi}_3\text{O}(\text{OH})(\text{PO}_4)_2$ at 298 K, while further increasing the pH leads to the precipitation of compounds with similar solubility, such as Bi_2O_3 , BiOOH , or $\text{Bi}(\text{OH})_3$ at 298 and 473 K. Overall, the thermodynamic calculation is in satisfactory agreement with the experimental data obtained.

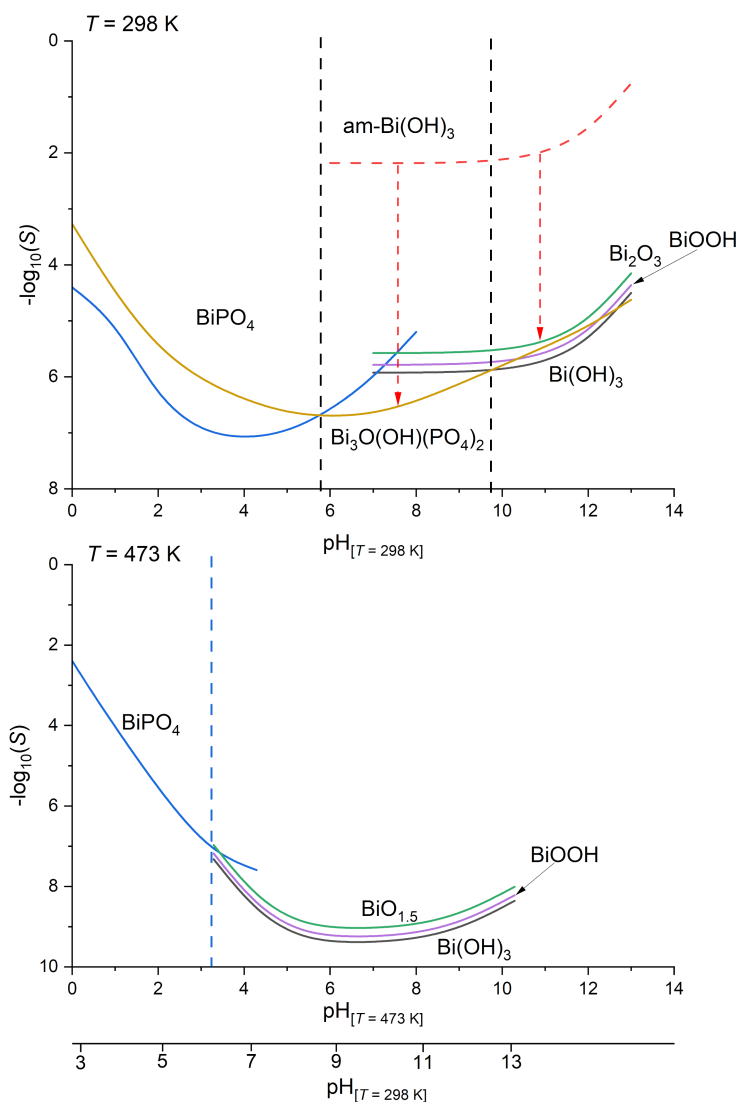


FIG. 3. Dependence of the equilibrium molar solubility (S , mol/L) of solid BiPO_4 , Bi(OH)_3 , $\text{BiO}_{1.5}$, BiOOH and $\text{Bi}_3\text{O(OH)(PO}_4)_2$ in a aqueous-salt suspension on pH at temperatures 298 and 473 K

References

- [1] Diodati S., Walton R.I., Mascotto S., Gross S. Low-temperature wet chemistry synthetic approaches towards ferrites. *Inorganic Chemistry Frontiers*, 2020, **7** (18), P. 3282–3314.
- [2] Bretos I., Jimenez R., Ricote J., Calzada M.L. Low-temperature crystallization of solution-derived metal oxide thin films assisted by chemical processes. *Chemical Society Reviews*, 2018, **47** (2), P. 291–308.
- [3] Diodati S., Dolcet P., Casarin M., Gross S. Pursuing the Crystallization of Mono- and Polymetallic Nanosized Crystalline Inorganic Compounds by Low-Temperature Wet-Chemistry and Colloidal Routes. *Chemical Reviews*, 2015, **115** (20), P. 11449–11502.
- [4] Gusarov V.V. Fast Solid-Phase Chemical Reactions. *Russ. J. Gen. Chem.*, 1997, **67** (12), P. 1846–1851.
- [5] Abiev R.S., Proskurina, O.V., Enikeeva, M.O., Gusarov V.V. Effect of Hydrodynamic Conditions in an Impinging-Jet Microreactor on the Formation of Nanoparticles Based on Complex Oxides. *Theor. Found. Chem. Eng.*, 2021, **55** (1), P. 12–29.
- [6] Almjasheva O.V., Popkov V.I., Proskurina O.V., Gusarov V.V. Phase formation under conditions of self-organization of particle growth restrictions in the reaction system. *Nanosystems: Phys. Chem. Math.*, 2022, **13** (2), P. 164–180.
- [7] Ghanizadeh S., Bao X., Vaidhyanathan B., Binner J. Synthesis of nano α -alumina powders using hydrothermal and precipitation routes: a comparative study. *Ceramics Int.*, 2014, **40** (1), P. 1311–1319.
- [8] Jesus A.C.B., Jesus J.R., Lima R.J.S., Moura K.O., Almeida J.M.A., Duque J.G.S., Meneses C.T. Synthesis and magnetic interaction on concentrated Fe_3O_4 nanoparticles obtained by the co-precipitation and hydrothermal chemical methods. *Ceramics Int.*, 2020, **46** (8), P. 11149–11153.
- [9] Gahrouei Z.E., Imani M., Soltani M., Shafyei A. Synthesis of iron oxide nanoparticles for hyperthermia application: Effect of ultrasonic irradiation assisted co-precipitation route. *Adv. Nat. Sci.: Nanosci. Nanotechnol.*, 2020, **11** (2), 025001.
- [10] Dehghanhadikolaei A., Ansary J., Ghoreishi R. Sol-gel process applications: A mini-review. *Proc. Nat. Res. Soc.*, 2018, **2** (1), P. 02008–02029.
- [11] Danks A.E., Hall S.R., Schnepf Z. The evolution of ‘sol-gel’ chemistry as a technique for materials synthesis. *Materials Horizons*, 2015 **3** (2), P. 91–112.

- [12] Verma S., Rani S., Kumar S. Crystal structure, morphology and optical behaviour of sol-gel derived pyrochlore rare earth titanates $\text{RE}_2\text{Ti}_2\text{O}_7$ (RE= Dy, Sm). *J. of Alloys and Compounds*, 2018, **750**, P. 902–910.
- [13] Bokov D., Jalil A.T., Chupradit S., Suksatan W., Ansari M.J., Shewael I.H., Valiev G.H., Kianfar E. Nanomaterial by sol-gel method: synthesis and application. *Advances in Materials Science and Engineering*, 2021, **2021**.
- [14] Ivanets A.I., Kuznetsova T.F., Prozorovich V.G. Sol-gel synthesis and adsorption properties of mesoporous manganese oxide. *Russian J. of Physical Chemistry A*, 2015, **89**, P. 481–486.
- [15] Berezhnaya M.V., Al'myasheva O.V., Mittova V.O., Nguen A.T., Mittova I.Y. Sol-gel synthesis and properties of $\text{Y}_{1-x}\text{Ba}_x\text{FeO}_3$ nanocrystals. *Russian J. of General Chemistry*, 2018, **88**, P. 626–631.
- [16] Filippova A.D., Rumyantsev A.A., Baranchikov A.E., Kolesnik I.V., Ivanova O.S., Efimov N.N., Khoroshilov A.V., Ivanov V.K. Hydrothermal Synthesis of $\gamma\text{-WO}_3$ and $h\text{-WO}_3$ Powders in the Presence of Citric Acid and Their Photoprotective Properties. *Russ. J. Inorg. Chem.*, 2022, **67** (6), P. 780–789.
- [17] Enikeeva M.O., Proskurina O.V., Gerasimov E.Yu., Nevedomskiy V.N., Gusarov V.V. Synthesis under hydrothermal conditions and structural transformations of nanocrystals in the $\text{LaPO}_4\text{-YPO}_4\text{-(H}_2\text{O)}$ system. *Nanosystems: Phys. Chem. Math.*, 2023, **14** (6), P. 660–671.
- [18] Lomakin M.S., Proskurina O.V., Gusarov V.V. Pyrochlore phase in the $\text{Bi}_2\text{O}_3\text{-Fe}_2\text{O}_3\text{-WO}_3\text{-(H}_2\text{O)}$ system: its formation by hydrothermal synthesis in the low-temperature region of the phase diagram. *Nanosystems: Phys. Chem. Math.*, 2023, **14** (2), P. 242–253.
- [19] Bachina A.K., Almjashaeva O.V., Popkov V.I. Formation of ZrTiO_4 under Hydrothermal Conditions. *Russ. J. Inorg. Chem.*, 2022, **67**, P. 830–838.
- [20] Prabhakaran T., Mangalaraja R.V., Denardin J.C. Controlling the Size and Magnetic Properties of Nano CoFe_2O_4 by Microwave Assisted Co-Precipitation Method. *Materials Research Express*, 2018, **5** (2), 026102.
- [21] Ivanov V.K., Baranchikov A.E., Vanetsev A.S., Shaporev A.S., Polezhaeva O.S., Tretyakov Yu.D., Fedorov P.P., Osiko V.V. Effect of Hydrothermal and Ultrasonic/Hydrothermal Treatment on the Phase Composition and Micromorphology of Yttrium Hydroxocarbonate. *Russ. J. Inorg. Chem.*, 2007, **52** (9), P. 1321–1327.
- [22] Khrapova E.K., Kozlov, D.A., Krasilin A.A. Hydrothermal Synthesis of Hydrosilicate Nanoscrolls $(\text{Mg}_{1-x}\text{Co}_x)_3\text{Si}_2\text{O}_5(\text{OH})_4$ in a Na_2SO_3 Solution. *Russian J. of Inorganic Chemistry*, 2022, **67** (6), P. 839–849.
- [23] Enikeeva M.O., Proskurina O.V., Danilovich D.P., Gusarov V.V. Formation of nanocrystals based on equimolar mixture of lanthanum and yttrium orthophosphates under microwave-assisted hydrothermal synthesis. *Nanosystems: Phys. Chem. Math.*, 2020, **11** (6), P. 705–715.
- [24] Meskin P.E., Gavrilov A.I., Maksimov V.D., Ivanov V.K., Churagulov B.P. Hydrothermal/microwave and hydrothermal/ultrasonic synthesis of nanocrystalline titania, zirconia, and hafnia. *Russian J. of Inorganic Chemistry*, 2007, **52**, P. 1648–1656.
- [25] Amin G., Asif M.H., Zainelabdin A., Zaman S., Nur O., Willander M. Influence of pH, Precursor Concentration, Growth Time, and Temperature on the Morphology of ZnO Nanostructures Grown by the Hydrothermal Method. *J. of Nanomaterials*, 2011, **2011**, 269692.
- [26] Zhang A., Zhang J., Cui N., Tie X., An Y., Li L. Effects of pH on Hydrothermal Synthesis and Characterization of Visible-Light-Driven BiVO_4 Photocatalyst. *J. Mol. Catal. A: Chem.*, 2009, **304** (1–2), P. 28–32.
- [27] Shojaei N., Ebadzadeh T., Aghaei A. Effect of Concentration and Heating Conditions on Microwave-Assisted Hydrothermal Synthesis of ZnO Nanorods. *Mater. Charact.*, 2010, **61** (12), P. 1418–1423.
- [28] Solomatin S.V., Bronich T.K., Bargar T.W., Eisenberg A., Kabanov V.A., Kabanov A.V. Environmentally responsive nanoparticles from block ionomer complexes: effects of pH and ionic strength. *Langmuir*, 2003, **19** (19), P. 8069–8076.
- [29] Belous A.G., Pashkova E.V., Elshanskii V.A., Ivanitskii V.P. Effect of precipitation conditions on the phase composition, particle morphology, and properties of iron (III, II) hydroxide precipitates. *Inorganic Materials*, 2000, **36**, P. 343–351.
- [30] Lomakin M.S., Proskurina O.V., Gusarov V.V. Influence of hydrothermal synthesis conditions on the composition of the pyrochlore phase in the $\text{Bi}_2\text{O}_3\text{-Fe}_2\text{O}_3\text{-WO}_3$ system. *Nanosystems: Phys. Chem. Math.*, 2020, **11** (2), P. 246–251.
- [31] Du X., Wang Y., Su X., Li, J. Influences of pH value on the microstructure and phase transformation of aluminum hydroxide. *Powder Technology*, 2009, **192** (1), P. 40–46.
- [32] Alam M.A., Bishwas R.K., Mostofa S., Jahan S.A. Crystallographic phase stability of nanocrystalline polymorphs TiO_2 by tailoring hydrolysis pH. *South African J. of Chemical Engineering*, 2024, **49**, P. 73–85.
- [33] Zhang H., Zhang X., Graham T.R., Pearce C.I., Hlushko H., LaVerne J.A., Liu L., Wang S., Zheng S., Clark S.B., Li P., Wang Z., Rosso K.M. Crystallization and phase transformations of aluminum (oxy) hydroxide polymorphs in caustic aqueous solution. *Inorganic Chemistry*, 2021, **60** (13), P. 9820–9832.
- [34] Kozerozhets I.V., Semenov E.A., Avdeeva V.V. Ivakin Y.D., Kuprenko S.Y., Egorov A.V., Kholodkova A.A., Vasil'ev M.G., Kozlova L.O., Panasyuk G.P. State and forms of water in dispersed aluminum oxides and hydroxides. *Ceramics Int.*, 2023, **49** (18), P. 30381–30394.
- [35] Enikeeva M.O., Kenges K.M., Proskurina O.V., Danilovich D. P., Gusarov V.V. Influence of hydrothermal treatment conditions on the formation of lanthanum orthophosphate nanoparticles of monazite structure. *Russian J. of Applied Chemistry*, 2020, **93**, P. 540–548.
- [36] Li N., Yanagisawa K. Controlling the Morphology of Yttrium Oxide through Different Precursors Synthesized by Hydrothermal Method. *J. Solid State Chem.*, 2008, **181** (8), P. 1738–1743.
- [37] Lu C.H., Yeh C.H. Influence of hydrothermal conditions on the morphology and particle size of zinc oxide powder. *Ceramics Int.*, 2000, **26** (4), P. 351–357.
- [38] Khrapova E.K., Kozlov D., Krasilin A.A. Hydrothermal Synthesis of Hydrosilicate Nanoscrolls $(\text{Mg}_{1-x}\text{Co}_x)_3\text{Si}_2\text{O}_5(\text{OH})_4$ in a Na_2SO_3 Solution. *Russ. J. Inorg. Chem.*, 2022, **67**, P. 839–849.
- [39] Skachkov V.M., Pasechnik L.A., Medyankina I.S. Hydrothermal Synthesis of Calcium Silicates on the Recovery of Phosphorus from Phosphorite. *Russian J. of Inorganic Chemistry*, 2023, **68** (11), P. 1532–1536.
- [40] Chithra M.J., Sathya M., Pushpanathan K. Effect of pH on crystal size and photoluminescence property of ZnO nanoparticles prepared by chemical precipitation method. *Acta Metallurgica Sinica (English Letters)*, 2015, **28**, P. 394–404.
- [41] Syukkalova E.A., Sadetskaya A.V., Demidova N.D., Bobrysheva N.P., Osmolowsky M.G., Voznesenskiy M.A., Osmolovskaya O.M. The effect of reaction medium and hydrothermal synthesis conditions on morphological parameters and thermal behavior of calcium phosphate nanoparticles. *Ceramics Int.*, 2021, **47** (2), P. 2809–2821.
- [42] Obolenskaya L.N., Kuz'micheva G.M., Savinkina E.V., Sadvokskaya N.V., Zhilkina A.V., Prokudina N.A., Chernyshev V.V. Influence of the conditions of the sulfate method on the characteristics of nanosized anatase-type samples. *Russian Chemical Bulletin*, 2012, **61**, P. 2049–2055.
- [43] Proskurina O.V., Sokolova A.N., Sirotkin A.A., Abiev R.S., Gusarov V.V. Role of hydroxide precipitation conditions in the formation of nanocrystalline BiFeO_3 . *Russian J. of Inorganic Chemistry*, 2021, **66**, P. 163–169.
- [44] Uskoković V. Disordering the disorder as the route to a higher order: incoherent crystallization of calcium phosphate through amorphous precursors. *Crystal Growth & Design*, 2019, **19** (8), P. 4340–4357.
- [45] Gómez L.R., Vega, D.A. Amorphous precursors of crystallization during spinodal decomposition. *Physical Review E*, 2011, **83** (2), 021501.

- [46] Vallina B., Rodriguez-Blanco J.D., Brown A.P., Blanco J.A., Benning L.G. The role of amorphous precursors in the crystallization of La and Nd carbonates. *Nanoscale*, 2015, **7** (28), P. 12166–12179.
- [47] Krasilin A.A., Almjasheva O.V., Gusarov V.V. Effect of the structure of precursors on the formation of nanotubular magnesium hydrosilicate. *Inorg. Mater.*, 2011, **47** (10), 1111.
- [48] Popkov V.I., Almjasheva O.V., Schmidt M.P., Gusarov V.V. Formation mechanism of nanocrystalline yttrium orthoferrite under heat treatment of the coprecipitated hydroxides. *Russ. J. Gen. Chem.*, 2015, **85** (6), P. 1370–1375.
- [49] Galanov S.I., Sidorova O.I. Effect of a precursor on the phase composition and particle size of the active component of Ni-ZrO₂ catalytic systems for the oxidation of methane into syngas. *Russian J. of Physical Chemistry A*, 2014, **88**, P. 1629–1636.
- [50] Almjasheva O.V., Krasilin A.A., Gusarov V.V. Formation mechanism of core-shell nanocrystals obtained via dehydration of coprecipitated hydroxides at hydrothermal conditions. *Nanosystems: Phys. Chem. Math.*, 2018, **9** (4), P. 568–572.
- [51] Yang G., Park S.J. Conventional and microwave hydrothermal synthesis and application of functional materials: A review. *Materials*, 2019, **12** (7), 1177.
- [52] Almjasheva O.V., Gusarov V.V. Prenucleation Formations in Control over Synthesis of CoFe₂O₄ Nanocrystalline Powders. *Russian J. of Applied Chemistry*, 2016, **89** (6), P. 851–856.
- [53] Abiev R.Sh. Impinging-Jets Micromixers and Microreactors: State of the Art and Prospects for Use in the Chemical Technology of Nanomaterials (Review). *Theor. Found. Chem. Eng.*, 2020, **54**, P. 1131–1147.
- [54] Abiev R.S., Nikolaev A.M., Kovalenko A.S., Tsvigun N.V., Baranchikov A.E., Kopitsa G.P., Shilova O.A. One step synthesis of FeO_x magnetic nanoparticles in the microreactor with intensively swirling flows. *Chemical Engineering Research and Design*, 2024, **205**, P. 335–342.
- [55] Abiev R.S., Almjasheva O.V., Popkov V.I., Proskurina O.V. Microreactor synthesis of nanosized particles: The role of micromixing, aggregation, and separation processes in heterogeneous nucleation. *Chemical Engineering Research and Design*, 2022, **178**, P. 73–94.
- [56] Wang Y., Guan X., Li L., Li G. pH-driven hydrothermal synthesis and formation mechanism of all BiPO₄ polymorphs. *Cryst. Eng. Comm.*, 2012, **14** (23), P. 7907–7914.
- [57] Elovikov D.P., Nikiforova K.O., Tomkovich M.V., Proskurina O.V., Gusarov V.V. The pH value influence on the waylandite-structured BiAl₃(PO₄)₂(OH)₆ compound formation under hydrothermal conditions. *Inorganica Chimica Acta*, 2024, **561**, 121856.
- [58] Achary S.N., Errandonea D., Muñoz A., Rodríguez-Hernández P., Manjón F.J., Krishna P.S.R., Patwe S.J., Grover V., Tyagi A.K. Experimental and theoretical investigations on the polymorphism and metastability of BiPO₄. *Dalton Transactions*, 2013, **42** (42), P. 14999–15015.
- [59] Zhao M., Li G., Zheng J., Li L., Wang H., Yang L. Preparation and polymorph-sensitive luminescence properties of BiPO₄: Eu, Part I: room-temperature reaction followed by a heat treatment. *Cryst. Eng. Comm.*, 2011, **13** (20), P. 6251–6257.
- [60] Sahu S.P., Qanbarzadeh M., Ateia M., Torkzadeh H., Maroli A.S., Cates E.L. Rapid degradation and mineralization of perfluorooctanoic acid by a new petitjeanite Bi₃O(OH)(PO₄)₂ microparticle ultraviolet photocatalyst. *Environmental Science & Technology Letters*, 2018, **5** (8), P. 533–538.
- [61] Bentel M.J., Mason M.M., Cates E.L. Synthesis of Petitjeanite Bi₃O(OH)(PO₄)₂ Photocatalytic Microparticles: Effect of Synthetic Conditions on the Crystal Structure and Activity toward Degradation of Aqueous Perfluorooctanoic Acid (PFOA). *ACS Applied Materials & Interfaces*, 2023, **15** (17), P. 20854–20864.
- [62] Eremin O.V., Yurgenson G.A., Solodukhina M.A., Epova E.S. Hypergene minerals of antimony and bismuth: a method for estimating their standard Gibbs potentials. *Mineralogy of technogenesis*, 2018, **19**, P. 103–131.
- [63] Shkol'nikov E.V., Elovikov D.P. Thermodynamic calculation of the effect of polymorphism and pH value on the solubility of aluminium oxide and its hydrates in aqueous media. *Izvestiya SPbLTA*, **231**, 2020, P. 209–221 (in Russian).
- [64] Tuan A.D. Low-temperature hydrothermal synthesis of BiPO₄ for Rhodamine B removal. *Vietnam J. of Catalysis and Adsorption*, 2022, **11** (3), P. 33–36.
- [65] Cheng L.W., Tsai J.C., Huang T.Y., Huang C.W., Unnikrishnan B., Lin Y.W. Controlled synthesis, characterization and photocatalytic activity of BiPO₄ nanostructures with different morphologies. *Materials Research Express*, 2014, **1** (2), 025023.
- [66] Shi X., Liu Y., Zhang J., Zhang K., Li P., Zuo H., Li J. Effects of pH and Sm³⁺ doping on the structure, morphology and luminescence properties of BiPO₄: Sm³⁺ phosphors prepared by hydrothermal method. *Ceramics Int.*, 2015, **41** (2), P. 3162–3168.

Submitted 29 April 2024; revised 30 May 2024; accepted 3 June 2024

Information about the authors:

Dmitry P. Elovikov – Grebenshchikov Institute of Silicate Chemistry, Russian Academy of Sciences, St. Petersburg, Russia, 197022, St. Petersburg, Russia; ORCID 0000-0003-4345-6086; syncdima@mail.ru

Alena A. Osminina – Grebenshchikov Institute of Silicate Chemistry, Russian Academy of Sciences, St. Petersburg, Russia, 197022, St. Petersburg, Russia; ORCID 0009-0008-8804-4732; alenaosminina3001@gmail.com

Conflict of interest: the authors declare no conflict of interest.